Analysis of the optics of the AUGER mirrors

P. W. Cattaneo

INFN Pavia, Via Bassi 6 - 27100, Pavia, Italy
Email: Paolo.Cattaneo@pv.infn.it

Abstract

The light distribution on the focal surface of the AUGER mirrors is calculated analytically in various configurations using geometrical optics.

1 Introduction

The lens-less Schimdt camera is the baseline design for the optics of the AUGER Fluorescence detector. With a diaphragm in the center of curvature the coma aberration is a second order effect and the dominant aberration is spherical. We are primarily interested in calculating the light distribution on the spherical focal surface for application to detector simulation. //This calculation can also be useful for finalizing the design of the mirror.

In Fig.1 the schematic of an AUGER FD mirror is drawn with an appropriate reference frame. It differs from the one used in [1] in the origin and the direction of the z axis.
The mirror is is a spherical sector with radius $R_M = 3400$ mm and with edges $R_M = 3400$ mm.
The light entrance is limited from a circular diaphragm centered in the mirror center with radius $R_d = 850$ mm, that defines and effective semiaperture of angle $\sin\Theta_M = R_d/R_M$.
Using geometrical optics the light distribution on the focal plane due to paraxial rays is calculated and the roles of the camera obscuration is estimated.

2 Light profile from paraxial rays without obscuration

We consider a ray parallel to the z axis at distance $\rho \leq R_M \sin\Theta_M$. The use of the radial parameter ρ is justified by the cilindrical simmetry of the

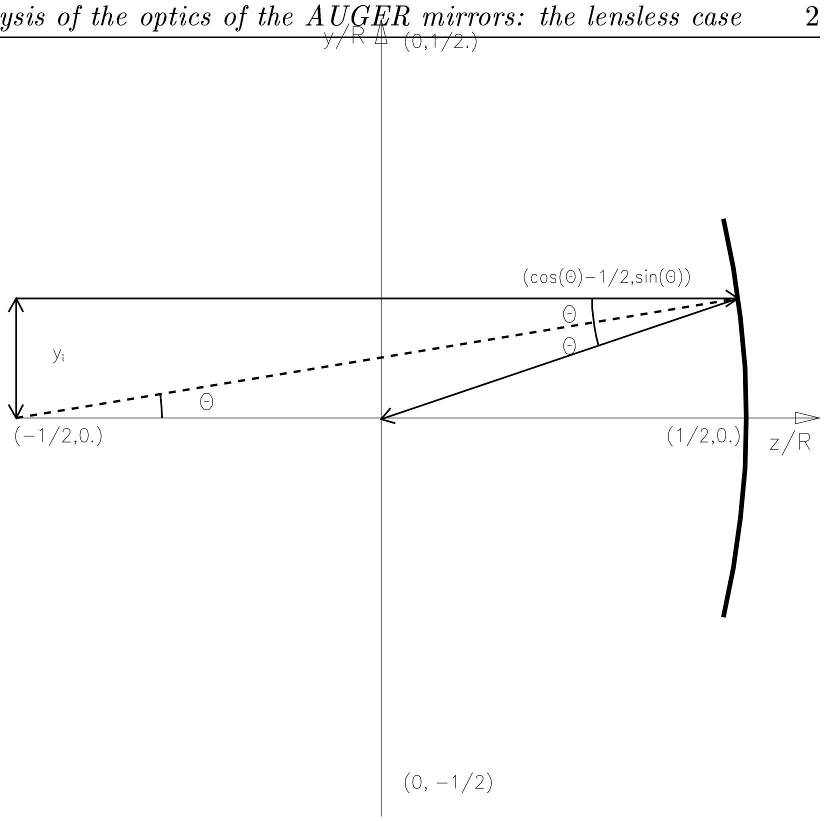

Figure 1: Schematic of the mirror with the reference frame.

problem. In Fig.1, representing the $y - z$ plane, ρ coincides with the y coordinate.
The ray intercept the mirror at the point $(R_M(\cos\Theta - \frac{1}{2}), R_M \sin\Theta)$ where Θ is the angle of the point with respect to the circle center (not the axis origin). The reflected rays form an angle 2Θ with the z axis and its equation is

$$\begin{aligned} \rho - R_M \sin\Theta &= \tan 2\Theta \left(z - R_M \left(\cos\Theta - \frac{1}{2} \right) \right) \\ \rho &= \tan 2\Theta \left(z + \frac{R_M}{2} \left(1 - \frac{1}{\cos\Theta} \right) \right) \end{aligned} \tag{1}$$

This last form is equal to Eq.10 of [1].

2.1 Calculation of the caustic

As part of the calculation of the light distribution on the focal surface, it is useful to calculate preliminarly the caustic of the spherical surface. The relevant formulae are presented in the Appendix.
The relevance of the caustic on the calculation of the light distribution stems from the fact that, for $\sin\Theta \leq \sin\Theta_M$, it is the outer envelope of the converging rays. We are interested in studying the behaviour of the rays close to the focal point, where the previous condition on Θ is verified, therefore, as already pointed out in [1] the outer diameter of the light disk is the maximum between the radial coordinate of the caustic and of the rays from the mirror rim, that is Eq.1 for $\Theta = \Theta_M$.

2.2 Light envelope and disk of minimal confusion

To calculate the size and the amplitude of the disk, the equation of the caustic is reformulated and the following system must be calculated

$$\begin{aligned} \frac{z}{R_M} &= \frac{1}{2} \left[-1 + \sqrt{1 - (\frac{\rho}{R_M})^{\frac{2}{3}}} (1 + 2(\frac{\rho}{R_M})^{\frac{2}{3}}) \right] \\ \frac{\rho}{R_M} &= \tan 2\Theta_M \left(\frac{z}{R_M} + \frac{1}{2}(1 - \frac{1}{\cos\Theta_M}) \right) \end{aligned} \tag{2}$$

We can anticipate that the solution will be at small ρ, therefore we apply the approximation in Eq.16 and obtain the following third order polynomial equation

$$\left(\frac{z}{R_M}\right)^3 - \frac{27}{64} \tan^2(2\Theta_M) \left[\left(\frac{z}{R_M}\right)^2 + \left(\frac{z}{R_M}\right) \left(1 - \frac{1}{\cos\Theta_M}\right) + \frac{1}{4} \left(1 - \frac{1}{\cos\Theta_M}\right)^2 \right] = 0 \tag{3}$$

that can be solved with the usual Cardano method. We remark that the reflected ray from the largest angle Θ_M (mirror rim or diaphragm delimited circle) touches the caustic in two points: it is tangent in the first, at larger z, by definition of caustic and has a simple intersection in the second, at smaller z, that is the one giving the disk of minimal confusion, given by

$$p = -\frac{27}{64}\tan^2 2\Theta_M \left[(1 - \frac{1}{\cos\Theta_M}) + \frac{9}{64}\tan^2 2\Theta_M \right]$$

$$q = \frac{2}{27}\left[-\frac{27}{64}\tan^2 2\Theta_M\right]^3 - \frac{1}{3}\left[-\frac{27}{64}\tan^2 2\Theta_M\right]^2 (1-\frac{1}{\cos\Theta_M}) - \frac{27}{64}\tan^2 2\Theta_M (1-\frac{1}{\cos\Theta_M})^2$$

$$\frac{z_{dm}}{R_M} = \sqrt[3]{-\frac{q}{2} + \sqrt{\frac{p^3}{27} + \frac{q^2}{4}}} + \sqrt[3]{-\frac{q}{2} - \sqrt{\frac{p^3}{27} + \frac{q^2}{4}}} + \frac{9}{64}\tan^2(\Theta_M) \qquad (4)$$

In Fig.2 the envelope of light rays next to the mirror focus is pictured with the caustic and some rays from the mirror. The outer envelope is given by the rays converging from the outer rims for

$$\frac{1}{2}(-1 + \sqrt{1 - \sin^2\Theta_M}(1 + 2\sin^2\Theta_M)) \le \frac{z}{R_M}$$

by the caustic for

$$\frac{z_{dm}}{R_M} \le \frac{z}{R_M} \le \frac{1}{2}(-1 + \sqrt{1 - \sin^2\Theta_M}(1 + 2\sin^2\Theta_M))$$

(where z_{dm} is the position of the disk of minimal confusion obtained by Eq.3) and by the rays diverging from the outer rims for

$$\frac{z}{R_M} \le \frac{z_{dm}}{R_M}.$$

The radius of the envelope versus the radial distance is displayed in Fig. 3 (solid line) for the case $R_M = 3400\,mm$.
For the AUGER mirror design the position of the disk of minimal confustion is $R = 1742.52mm$ and its radius is $7.32mm$.

2.3 Light distribution

To calculate the radial light distribution $\frac{df}{d\rho}$ at fixed z, we must relate the known light distribution in ρ_i with that in ρ. The relations stems from

$$\frac{df}{d\rho} = \frac{df}{d\Theta}\frac{d\Theta}{d\rho} = \frac{df}{d\rho_i}\frac{d\rho_i}{d\Theta}\frac{d\Theta}{d\rho} = \frac{df}{dA}\frac{dA}{d\rho_i}\frac{d\rho_i}{d\Theta}\frac{d\Theta}{d\rho} \qquad (5)$$

The first factor is simply the inverse of the effective area of the mirror $\frac{df}{dA} = (\pi R_M^2 \sin^2\Theta_M)^{-1}$, the second is simply $\frac{dA}{d\rho_i} = 2\pi\rho_i$, the third, from

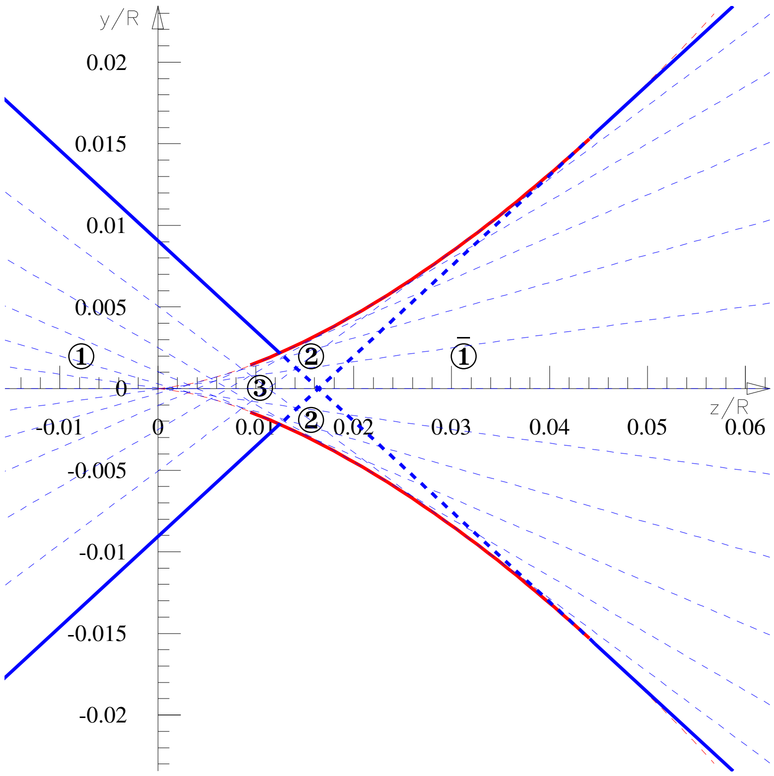

Figure 2: Envelope of light rays next to the focus. Thick lines are external, dashed internal.

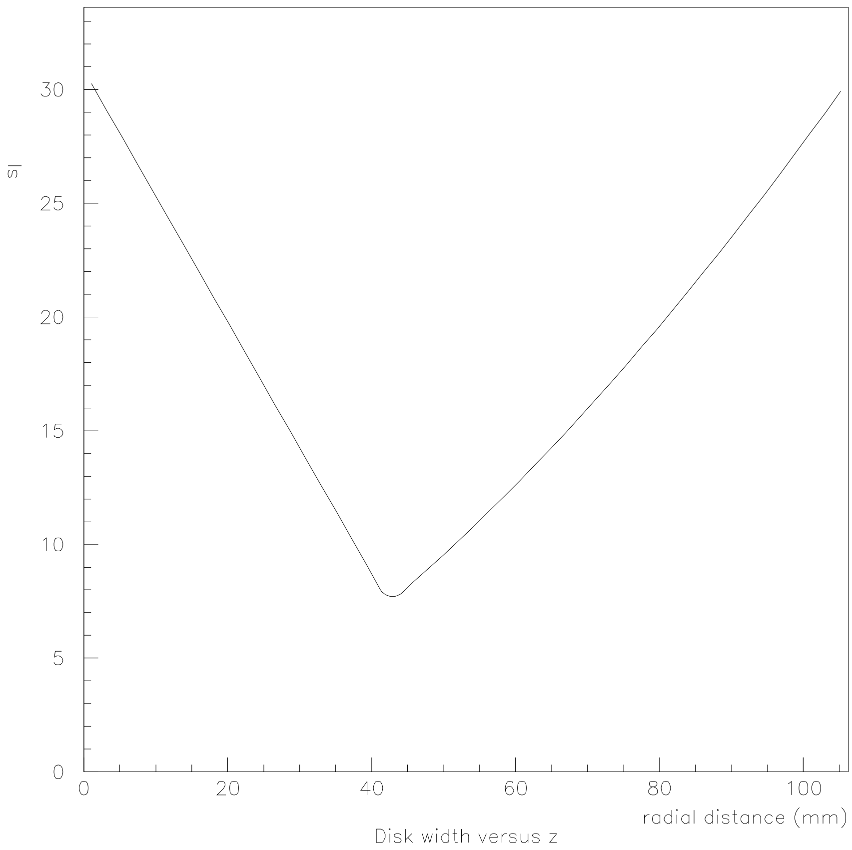

Figure 3: Spot radius versus radial distance from the focus: unobscured case (solid), obscured case (dashed).

$\rho_i = R_M \sin\Theta$, is $\frac{d\rho_i}{d\Theta} = R_M \cos\Theta$. The fourth must be derived from Eq.1: differentiating one obtains

$$\frac{d\Theta}{d(\rho/R_M)} = \frac{1}{\frac{2}{\cos^2 2\Theta}(z/R_M + \frac{1}{2}(1 - \frac{1}{\cos\Theta})) - \frac{\tan 2\Theta \sin\Theta}{2\cos^2\Theta}}$$

therefore Eq.5 can be written as

$$\frac{df}{d(\rho/R_M)} = \frac{2\pi \sin\Theta \cos\Theta}{\pi \sin^2\Theta_M} \frac{1}{\frac{2}{\cos^2 2\Theta}(z/R_M + \frac{1}{2}(1 - \frac{1}{\cos\Theta})) - \frac{\tan 2\Theta \sin\Theta}{2\cos^2\Theta}} \tag{6}$$

where Θ must be espressed as function of ρ_i inverting Eq.1.
The inversion requires the canonical change of variable $t = \tan\Theta/2$. In this new variable $\sin\Theta = \frac{2t}{1+t^2}$ and $\cos\Theta = \frac{1-t^2}{1+t^2}$, so that Eq.1 becomes

$$t^4 + \frac{4(z+1)}{\rho} t^3 - 6t^2 - \frac{4z}{\rho} t + 1 = 0 \tag{7}$$

From this equation we expect 4 complex solutions and 0, 2 or 4 of them can be real. That might appear a surprise, because the analysis of Fig.2 leads to the conclusion that in the region within the caustic and within the rays from the mirror rims after their crossing, three rays meets at a given ρ, one at small Θ that is converging and has not yet reached the caustic, one at larger Θ that is converging and that has already reached the caustic and one at even larger and opposite sign Θ that is diverging and has already reached the caustic on the opposite site; in the region within the caustic and outside the rays from the mirror rims, there are two rays, the diverging ray is missing; in the region within the caustic and within the rays from the mirror rims before their crossing, there is only the converging ray at small Θ that has not yet reached the caustic; in the region outside the caustic and outside the rays from the mirror rims, there are no rays.
The reason of this apparent contraddiction is that Eq.7 for $\rho > 0$ has always a solution for $t \leq -1$, that is $\Theta \leq -\pi/2$; and viceversa for $\rho < 0$. That corresponds to a ray refracted (not reflected) by an unphysical emisphere specular image around the ρ axis of the physical one. Said otherwise, Eq.1 represents full straight lines, while the reflected rays are only half straight lines. This solution is unphysical and must be neglected.
A simple analysis of Eq.7 leads to the conclusion that, for $\rho > 0$, there is always an additional real solution for $-1 < t < 0$ and a pair of solution that can be either both positive or complex conjugate.
The reason of the presence of a region with two solutions is simply that the solution at large and opposite sign Θ lays outside the physical region $(-\Theta_M, \Theta_M)$. For the same reason there is the region with one solution of converging ray at small Θ.
These two regions and the region with three physical solutions corresponds to the Eq.7 having four real solutions, the region with one physical solution

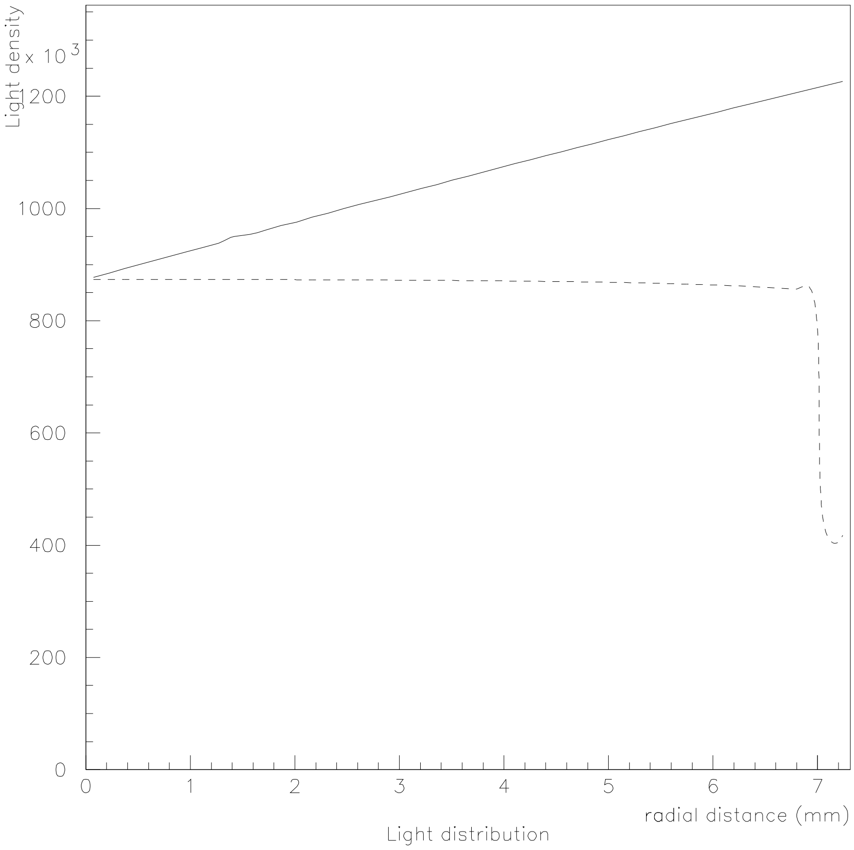

Figure 4: Radial light distribution at the disk of least confusion for unobscured (solid) and obscured (dashed) case

outside the caustic correspond to Eq.7 having two real and two complex solutions.
Eq.7 can be solved exactly using the canonical Ferrari approach. Nevertheless the solution is very cumbersome and little expressive. A slight approximation allows to reduce by one the order of the polynomial discarding the unphysical solution of the refracted ray. The ratio of the second and the fourth terms is $6/t^2$, where, at most, $t = \tan\Theta_M/2 \approx \Theta_M/2 \approx 1/8$; hence it is 384. That means that dropping the fourth power term will affect the solutions only of a very small amount. Under this approximation Eq.7 becomes

$$t^3 - \frac{6\rho}{4(z+1)}t^2 - \frac{z}{(z+1)}t + \frac{\rho}{4(z+1)} = 0 \tag{8}$$

The distribution $\frac{df}{d\rho}$ is plotted in Fig.4, that has to be compared with

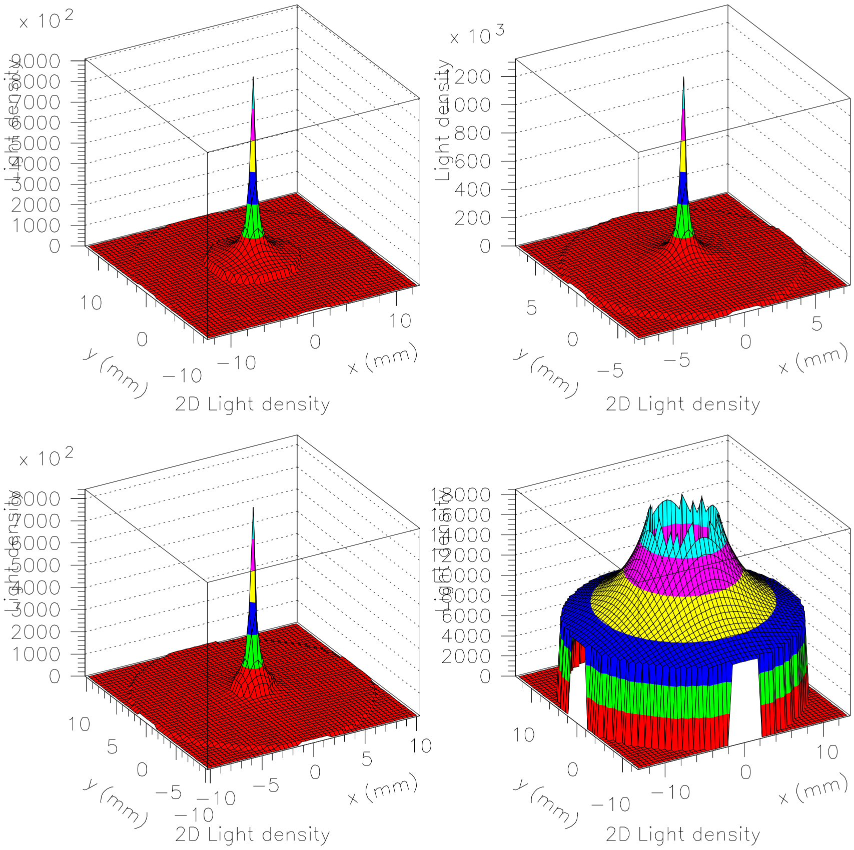

Figure 5: Two dimensional light distributions at -10, 0, +10, +20 mm from the plane of least confusion

Fig.2 of [2]. The two dimensional distribution is plotted in Fig.5 that has to be compared with Fig.9 of [1].

3 Light profile from paraxial rays with obscuration

The previous calculations assume ideally that there is no obscuration due to a camera next to the focus. In the AUGER design there is a photomultiplier camera with spherical surface next to focal plane with size $0.92 \times 0.92\ \mathrm{m}^2$. The camera does not have rotational simmetry but, following [1] the obscuration due to it is represented by a disk with the same area, that is with radius $R_c = 0.519\,\mathrm{m}$ positioned next to the focal plane $z = R_M/2$. That implies that the rays hit the mirror only for angle $\sin\Theta \geq \Theta_c = R_c/R_M$, that is for $\Theta \geq \Theta_c = 8.78^0$.

3.1 Light envelope and disk of minimal confusion

The obscuration changes the light distribution along z and might change the disk of minimal confusion. The reflected light outer profile can be deduced referring to Fig.1 just noting that the light rays close to the z axis are obscurated. Hence the outer profile of the converging rays is given by the converging rays from the mirror rims up to the caustic, then by the caustic, then, possibly, by the converging rays from the rims of the obscuration disk, then by the diverging rays from the mirror rims.
It depends on the obscuration area if the converging rays from the rims of the obscuration disk touches the caustic at $z_c(\Theta_c)$ before or after $z_{dm}(\Theta_M)$ from Eq.4, that is if

$$z_{dm}(\Theta_M) \geq \frac{1}{2}(-1 + \sqrt{1-\sin^2\Theta_c}(1+2\sin^2\Theta_c)) \approx \frac{3}{4}sin^2\Theta_c = z_c(\Theta_c)$$

where the caustic approximation of Eq.16 is used.
Therefore if $\sin\Theta_c \leq \sqrt{z_{dm}(\Theta_M)4/3}$, the outer profile does not change, otherwise for $z_{dm} < z < z_c$ it is given by the converging rays from the rim of the obscuration disk. In this last case the disk of minimal confusion is obtained intersecting the diverging ray from the outer rim with the converging one on the opposite side from the rim of the obscuration disk. The result is

$$\begin{aligned} z_{dm} &= \frac{1}{2}\left(-1 + \left(\frac{\tan 2\Theta_M}{\cos\Theta_M} + \frac{\tan 2\Theta_c}{\cos\Theta_c}\right)\frac{1}{\tan 2\Theta_c + \tan 2\Theta_M}\right) \\ \rho_{dm} &= \frac{\tan 2\Theta_c}{2}\left(\left(\frac{\tan 2\Theta_c}{\cos\Theta_M} + \frac{\tan 2\Theta_c}{\cos\Theta_c}\right)\frac{1}{\tan 2\Theta_M + \tan 2\Theta_c} - \frac{1}{\cos\Theta_c}\right) \end{aligned} \quad (19)$$

In the AUGER mirror design this condition is verified and that changes slightly the location of the disk of minimal confusion. The position is

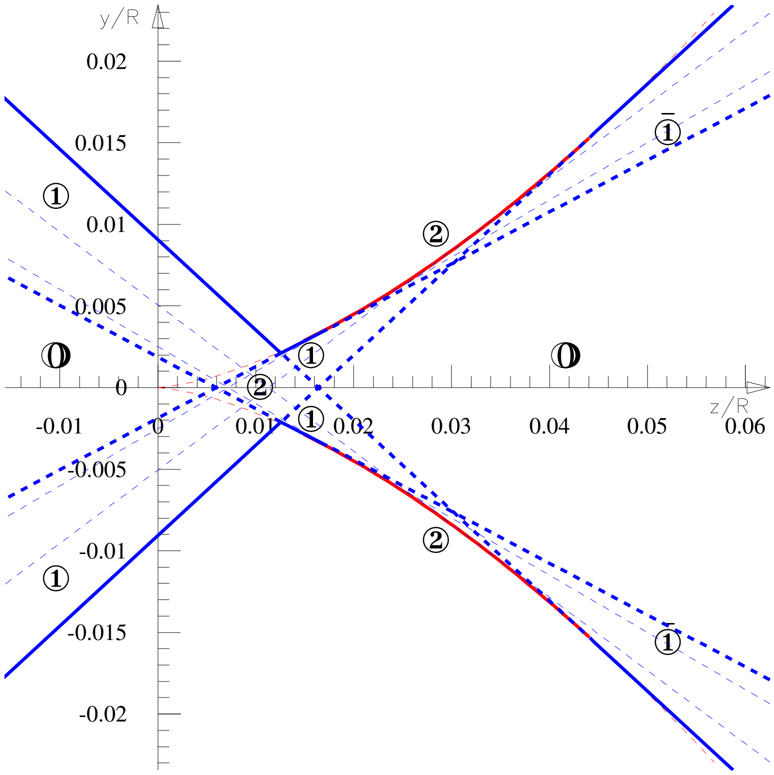

Figure 6: Envelope of light rays next to the focus with obscuration. Thick lines are external, dashed internal.

R = 1742.80 mm and its radius is 7.17 mm. The radius of the envelope versus the radial distance for the obscured case is displayed in Fig.3 (dashed line) for the AUGER design parameters. The differences with the unobscured case are minimal.

3.2 Light distributions

The consideration of the unobscured case applies, provided that only solutions with $\Theta_c \leq |\Theta| \leq \Theta_M$ are considred.
The radial light distribution for the obscured case is plotted in Fig.4 together with the unobscured case.

Appendix

Third order equation

We recall briefly some points on the solution of the polynomial third order equation. In the following the original form of the equation and the intermediate steps leading to the three solutions x_1, x_2 and x_3 are listed (where $\omega = \sqrt[3]{1}$, $\omega \neq 1$)

$$0 = x^3 + a_1 x^2 + a_2 x + a_3$$

$$p = a_2 - \frac{a_1^2}{3} \qquad q = \frac{2a_1^3}{27} - \frac{a_1 a_2}{3} + a_3$$

$$P = \sqrt[3]{-\frac{q}{2} + \sqrt{\frac{p^3}{27} + \frac{q^2}{4}}}$$

$$Q = \sqrt[3]{-\frac{q}{2} - \sqrt{\frac{p^3}{27} + \frac{q^2}{4}}}$$

$$x_1 = P + Q - \frac{a_1}{3} \quad x_2 = \omega P + \omega^2 Q - \frac{a_1}{3} \quad x_3 = \omega^2 P + \omega Q - \frac{a_1}{3} \tag{10}$$

It is easy to see that two roots coincides if and only if $\frac{p^3}{27} + \frac{q^2}{4} = 0$. In this case, the third distinct root is x_1. Hence for our application that is the solution determining the disk of least confusion.

Some formulae about the caustic

The calculation of the analytical form of the caustic from a spherical surface is a standard calculation, but it is surprisingly difficult to find on stantard text books its analytical form. Following a suggestion from [3] the caustic is the locus of intersection of neighbouring reflected rays when their distance becomes infinitesimal. Referring to the coordinate system in Eq.1 and using adimensional variables z and y, it can be calculated equating to 0 the derivative of Eq.1 with respect to the parameter Θ and solving the resulting system

$$\begin{aligned} y &= \tan 2\Theta \left(z + \frac{1}{2}\left(1 - \frac{1}{\cos\Theta}\right)\right) \\ 0 &= \frac{2}{\cos^2 2\Theta}\left(z + \frac{1}{2}\left(1 - \frac{1}{\cos\Theta}\right)\right) - \frac{1}{2}\frac{\tan 2\Theta \tan\Theta}{\cos\Theta} \end{aligned} \tag{11}$$

The resulting curve can be espressed in parametric form as

$$\begin{aligned} y(\Theta) &= \sin^3\Theta \\ z(\Theta) &= \frac{1}{2}(-1+\sqrt{1-\sin^2\Theta}(1+2\sin^2\Theta)) \end{aligned} \tag{12}$$

That differs by Eq. 7 from [1] partially for a different choice of reference system, partially (the factor 2 in front of the last $\sin^2\Theta$) because of a misprint in [1]. The three dimensional caustic is obtained rotating the curve in Eq.12 around the z axis.
It is useful to express exactly the caustic in alternative forms as $z(y)$, $y(z)$ and relating the parameter Θ to y and z. From Eq.12, we easily obtain

$$\begin{aligned} \Theta(y) &= \arcsin(\sqrt[3]{y}) \\ z(y) &= \frac{1}{2}(-1+\sqrt{1-y^{2/3}}(1+2y^{2/3})). \end{aligned} \tag{13}$$

A common and useful approximation for small Θ (that is equivalent to small y and small z) is obtained taking $\sqrt{1-y^{\frac{2}{3}}} = 1-\frac{1}{2}y^{\frac{2}{3}}$, that gives the additional expressions

$$z(y) = \frac{3}{4}y^{\frac{2}{3}} \tag{14}$$

$$y(z) = \pm(\frac{4z}{3})^{\frac{3}{2}} \tag{15}$$

$$\Theta(z) = \pm\arcsin\left(\sqrt{\frac{4z}{3}}\right) \tag{16}$$

The exact expression of $y(z)$ or, equivalently, of $\Theta(z)$ is obtained by Eq.12 writing

$$z(\Theta) = \frac{1}{2}(-1+\cos\Theta(3-2\cos^2\Theta))$$

that can be reformulated as

$$\cos^3\Theta - \frac{3}{2}\cos\Theta + (z+\frac{1}{2}) = 0$$

that is a third order polynomial equation.
The discriminant of this equation is

$$\Delta = -\frac{1}{8}+\frac{1}{4}(z+\frac{1}{2})^2$$

that is negative for $-\frac{\sqrt{2}+1}{2} < z < \frac{\sqrt{2}-1}{2} = z_0$. For these z values, there are three real solutions:

$$
\begin{aligned}
\cos\Theta_1(z) &= \sqrt{2}\cos\left(\frac{3\pi + \arctan\left(\frac{\sqrt{2-4(z+\frac{1}{2})^2}}{2(z+\frac{1}{2})}\right)}{3}\right)\\
\cos\Theta_2(z) &= \sqrt{2}\cos\left(\frac{5\pi + \arctan\left(\frac{\sqrt{2-4(z+\frac{1}{2})^2}}{2(z+\frac{1}{2})}\right)}{3}\right)\\
\cos\Theta_3(z) &= \sqrt{2}\cos\left(\frac{\pi + \arctan\left(\frac{\sqrt{2-4(z+\frac{1}{2})^2}}{2(z+\frac{1}{2})}\right)}{3}\right) \qquad (17)
\end{aligned}
$$

To understand the physical meaning of these solutions, we can consider them for $z = 0$

$$
\begin{aligned}
\cos\Theta_1(0) &= \sqrt{2}\cos(\frac{11}{12}\pi) = -\frac{\sqrt{2}}{2}\sqrt{2+\sqrt{3}}\\
\cos\Theta_2(0) &= \sqrt{2}\cos(\frac{\pi}{4}) = 1\\
\cos\Theta_3(0) &= \sqrt{2}\cos(\frac{5}{12}\pi) = \frac{\sqrt{2}}{2}\sqrt{2-\sqrt{3}} \qquad (18)
\end{aligned}
$$

The first is unphysical because is larger than 1 in module, the second solution correspond to the tip of the caustic, the third is a large angle solution.
Depending on the quadrant, the solutions are always monotonical versus z either increasing (Θ_1 and Θ_3) or decreasing (Θ_2) within the range $-\frac{1}{2} \leq z \leq z_0$. The lower bound of the range is physical, the upper one comes from requiring three real solutions. For $z = z_0$, $\Theta_2 = \Theta_3 = \pi/4$ and for $z > z_0$, Θ_2 and Θ_3 become complex conjugate.
The solution relevant for the application to a mirror is therefore Θ_2 and we can write the exact alternative parametrizations of the caustic for $0 \leq z \leq z_0$

$$
\begin{aligned}
\Theta(z) &= \pm\arccos\left(\sqrt{2}\cos\left(\frac{5\pi + \arctan(\frac{\sqrt{2-4(z+\frac{1}{2})^2}}{2(z+\frac{1}{2})})}{3}\right)\right)\\
y(z) &= \pm\left(-\cos 2\left(\frac{5\pi + \arctan(\frac{\sqrt{2-4(z+\frac{1}{2})^2}}{2(z+\frac{1}{2})})}{3}\right)\right)^{\frac{3}{2}}
\end{aligned}
$$

The large angle solution is Θ_3 and reads

$$\Theta(z) = \pm \arccos\left(\sqrt{2}\cos\left(\frac{\pi + \arctan(\frac{\sqrt{2-4(z+\frac{1}{2})^2}}{2(z+\frac{1}{2})})}{3}\right)\right)$$

$$y(z) = \pm\left(-\cos 2\left(\frac{\pi + \arctan(\frac{\sqrt{2-4(z+\frac{1}{2})^2}}{2(z+\frac{1}{2})})}{3}\right)\right)^{\frac{3}{2}}$$

References

[1] M. Hrabovsky et al. The optical analysis of the proposed schmidt camera design. GAP-99-025.

[2] G. Matthiae and P. Privitera. The schmidt telescope with corrector plane. GAP-98-039.

[3] B. Rossi. *Ottica*, chapter 2.7. Masson Italia Editori, Milano, 1984.